25th ABCM International Congress of Mechanical Engineering
October 20-25, 2019, Uberlândia, MG, Brazil

COB-2019-88
DYNAMIC ANALYSIS OF WIND TURBINE TOWERS UNDER RANDOM WIND LOADING

Lucas Carminatti Foschiera[1]
Herbert Martins Gomes[2]
[1,2]Universidade Federal do Rio Grande do Sul. Programa de Pós-Graduação em Engenharia Mecânica, Av. Sarmento Leite, 425, sala 202, 2º. Andar, 90050-170, Porto Alegre, RS, Brazil.
e-mail: lucas.foschiera@gmail.com[1], herbert@mecanica.ufrgs.br[2]

Dodani Renan de Morais[3]
[1]Universidade Federal do Rio Grande do Sul. Programa e Pós-Graduação em Engenharia Civil, Av. Oswaldo Aranha, 99, 3º. Andar, Porto Alegre, 90035-190, RS, Brazil.
e-mail: dodarenan10@hotmail.com[3]

Abstract. *This work proposes a methodology to evaluate the dynamic behavior over time of wind turbine towers taking into account the effects of wind on its structural components (tower, nacelle, and blades). A model of generation of wind velocity signals correlated in time and space is adopted, following an usual von Karman Power Spectral Density which has parameters such as turbulence intensities and standard deviations of the wind speed fluctuations in the three directions, velocity profile with height, and decay coefficients of the coherence with the distance between the points of wind action. It is investigated whether the time domain or frequency domain analysis are adequate in terms of simulation time, accuracy and computational costs for the evaluation of RMS values of acceleration and displacement signals at specific points of the wind turbine as well as base reactions. Three-dimensional beam type finite elements are used to obtain loads such as shear, bending moments and torsion. The Newmark Method for integration is used in time domain simulations. In the frequency domain, the direct integration of specific power spectral densities (displacements, accelerations, etc.) by the trapezoidal rule is employed. Results for a typical simulation are investigated and compared in different situations of wind speed and wind parameters for the simulation of the dynamic behavior of the structure. The obtained results present similarities regarding natural frequencies, main modes of vibration and vibration magnitude with cases reported in the literature.*

Keywords: *wind turbines, Newmark method, frequency domain analysis, correlated wind field generation*

1. INTRODUCTION

The analysis of tower structures of wind generators present in wind farms is part of the design of these systems in an energy production chain. In Brazil, the investment in this field of energy generation has recently increased in face of the volatility of the marketplace of nonrenewable energy sources of coal and oil and due to the growing demand for energy.

Numerical analysis of the structural behavior over time as well as the behavior in the frequency domain are essential tools for an economic project of a wind generator. This is relevant when diverse combinations of loads must be foreseen by regulatory impositions or even more detailed analysis regarding the buckling and fatigue of structural elements due to oscillatory characteristics of the external actions (mainly wind) along service time. Many causes are reported to contribute to the wind turbine tower failure, such as: the rotor imbalance, failure in brake systems, fatigue of low and high cycles, crack propagation in openings, discontinuities among parts, defective blades, in addition to construction causes, lightnings, fire and fissures in parts of the components and inappropriate/underestimated reactions at the tower foundation (Ma et al, 2018).

The work aims to propose a methodology of analysis for the tower's structure of wind turbines in the time and frequency domains with the possibility of obtaining information about the stresses, natural frequencies, displacements, reactions at the foundations, etc. It will be achieved based on the generation of wind velocity time histories, defined by the wind spectral densities, and on the tower properties, simulated in a simplified manner using Finite Elements.

2. WIND TURBINE TOWERS

Wind turbine towers or wind generators are devices that have the function of converting the kinetic energy of the wind into some useful form of energy, usually electricity. They can be classified according to the orientation of its rotor axis,

as vertical or horizontal, being the horizontal ones the most commonly used. Modern systems in large scale are typically horizontal axis turbines of three blades that work together in sites called wind farms. The wind turbine towers are mainly composed of blades, rotor, nacelle, platform, tower, and foundation. Figure 1a shows a typical wind turbine tower with its principal components and Fig. 1b shows a discrete finite element model, as used in this study.

The tower is the structure which supports the nacelle and the rotor while also provides the necessary height for the most efficient use of the wind. The tower needs to offer sufficient strength to bear the stresses caused by the wind, the weight of the nacelle and rotor, the wind thrust, the imbalance while operating as well as its own weight.

Nowadays, the towers that are most commonly used for wind generators are the tubular ones. They are normally composed of conic segments that range from 20 to 30 meters of length, connected by internal bolted flange joints. The maximum lengths of the segments are defined by transportation and assemblage requirements. The prevalence of tubular towers in wind generators is basically due to three factors: ease of assemblage; safety and comfort in the access to the nacelle; and visual aspect esthetically less invasive to the landscapes where they are located. Because of its critical structural importance along with the fact that its cost corresponds to around 30% of the total wind generator cost, it is natural that there are great incentives to the precise dimensioning of the tower structure, so that it is possible to save revenues, minimizing the expenses, and to guarantee the integrity of the wind turbine tower through all of its service life.

The blades of the wind generators are built with steel and light materials such as polymers, and timber, to minimize the rotational inertia of the equipment. Their aerodynamic shape is designed to optimize the capture of wind energy and the range of wind speeds that they are able to operate in. For simplified simulations, the mechanical properties of the blade may be evaluated in each section of the blade, in such a manner that permits to obtain a compatible model regarding the stiffness and mass for the displacements and natural frequencies evaluation. This is made by approximations that equalize these properties to the ones of an equivalent section of bars (Rodriguéz et al., 2007; Malcolm et al., 2007; Ashuri et al., 2010). The stiffnesses in the direction and perpendicular to the borders and the torsional stiffness, as well as the density, are given as function of these parameters at the root of the blade and of the dimensionless distance to the root.

3. NUMERICAL ANALYSIS AND SIMULATION

3.1 Tower modeling

The wind turbine tower, in the context of the finite element method, is modeled by a system of differential equations for the three possible orthogonal directions, as presented in Eq. (1), where $\{\mathbf{F}(t)\}$ represents the load vector, $[\mathbf{M}]$ is the mass matrix of the structure, $[\mathbf{C}]$ the damping matrix and $[\mathbf{K}]$ is the stiffness matrix. 3D beam finite elements are used leading to the degree of freedom displacement vector $\{\boldsymbol{x}(t)\}$, $u, v, w, \theta_u, \theta_v, \theta_w$ and their derivatives $\{\dot{\boldsymbol{x}}(t)\}$, $\{\ddot{\boldsymbol{x}}(t)\}$.

$$[\mathbf{M}]\{\ddot{\boldsymbol{x}}(t)\} + [\mathbf{C}]\{\dot{\boldsymbol{x}}(t)\} + [\mathbf{K}]\{\boldsymbol{x}(t)\} = \{\mathbf{F}(t)\} \tag{1}$$

The solution of this second order system of differential equations is here accomplished in two different ways: by direct time integration using the Newmark Scheme resulting in time histories or by the frequency domain resulting in the Frequency Response functions (Newland, 1984). The wind turbine tower and the simplified model are shown in Fig. 1.

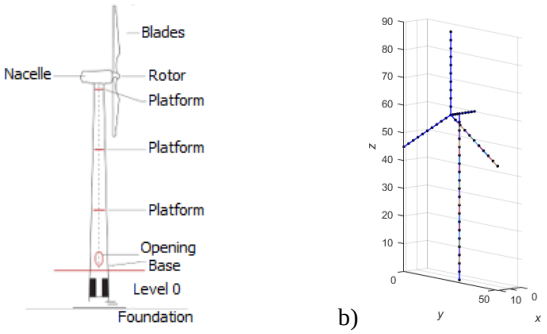

Figure 1. a) Main components of a wind turbine tower. b) Simplified finite element model.

3.2 Static analysis

Using the stiffness method, an equations system that determines the unknowns of the problem, such as displacements, reactions and stresses at each node, is solved. This method assumes the 3D elements of beams, which are linked through their nodes that have 6 degrees of freedom each. From the constitutive and compatibility equations, the individual behavior of each bar is expressed. Once the stiffness matrix is obtained, an adaptation from the local system of the elements to the global system of equilibrium equations is done. The typical equilibrium equations system of a 3D frame structure may be expressed as $[\mathbf{K}]\{\boldsymbol{x}\} = \{\mathbf{F}\}$, where $[\mathbf{K}]$ is the global stiffness matrix of the structure.

The stiffness matrix of an element in the global system of coordinates $[\mathbf{K}_e]$ is defined according to $[\mathbf{K}_e] = [\mathbf{T}]^T[\boldsymbol{k}][\mathbf{T}]$, with $[\mathbf{T}]$ being the rotational matrix and $[\boldsymbol{k}]$ the stiffness matrix of the element in the local system of coordinates. In order to obtain the global stiffness matrix of the structure $[\mathbf{K}]$ the assembling process is performed through the superposition of the matrices $[\mathbf{K}_e]$ using the numerical positions of their effective degrees of freedom.

3.3 Dynamic Analysis in the time domain

The mass matrix of the element is determined according to the consistent formulation and can be calculated based on the same transformation for the stiffness matrix. Using the expression of the kinetic energy associated to the element, the element's consistent mass matrix in the global system of coordinates is obtained $[\mathbf{M}_e] = [\mathbf{T}]^T[\boldsymbol{m}][\mathbf{T}]$**,** where $[\mathbf{M}_e]$ is the consistent mass matrix of the element in the global coordinate system, $[\mathbf{T}]$ is the transformational matrix and $[\boldsymbol{m}]$ is the consistent mass matrix in the local system.

The global mass matrix of the structure $[\mathbf{M}]$ is obtained the same way as the $[\mathbf{K}]$**.** A proportional damping model is implemented in such a way that the damping matrix $[\mathbf{C}]$ is diagonalizable with the modal matrix. At first, only the damping coefficients are specified for each mode of vibration and so $[\mathbf{C}]$ is calculated from the frequencies and modes of vibration, orthonormalized by the modal mass. For the solution of the coupled movement differential equations system, the Newmark implicit numerical integration method was used. Gyroscopic effects are neglected in this study since the analyzed situations are those with the stopped wind turbine due to high wind speeds.

3.4 Modal dynamic analysis in the frequency domain

The natural frequencies and modes of vibration of the system are computed based on the solution of an eigenvalues and eigenvectors problem, as shown in Eq. (2).

$$\left([\mathbf{K}] - \boldsymbol{\omega_i^2}[\mathbf{M}]\right)\{\boldsymbol{\varphi_i}\} = \mathbf{0} \tag{2}$$

In Eq. (2), $\boldsymbol{\omega_i}$ represents the *i*-th vibration frequencies (rad/s) and $\{\boldsymbol{\varphi_i}\}$ **vector** is the *i*-th modal shape. These vectors are orthonormalized, so that $\{\boldsymbol{\varphi}\}^T[\mathbf{M}]\{\boldsymbol{\varphi}\} = [\boldsymbol{I}]$ and $\{\boldsymbol{\varphi}\}^T[\mathbf{K}]\{\boldsymbol{\varphi}\} = [\boldsymbol{\Lambda}]$ holds, with $[\boldsymbol{I}]$ the identity matrix and diag($[\boldsymbol{\Lambda}]$)= $\{\omega_1^2, \dots, \omega_n^2\}^T$.

With the hypothesis of diagonalizable damping, i.e. $\{\boldsymbol{\varphi}\}^T[\mathbf{C}]\{\boldsymbol{\varphi}\} = diag(2\xi_1\omega_1, \dots, 2\xi_n\omega_n)$, the global damping matrix is determined as defined by Eq. (3).

$$[\mathbf{C}] = \{\boldsymbol{\varphi}\}^{-T}\begin{bmatrix} 2\xi_1\omega_1 & \cdots & 0 \\ \vdots & \ddots & \vdots \\ 0 & \cdots & 2\xi_n\omega_1 \end{bmatrix}\{\boldsymbol{\varphi}\}^{-1} = \{\boldsymbol{\varphi}\}^{-T}2[\mathbf{Z}][\boldsymbol{\Lambda}]\{\boldsymbol{\varphi}\}^{-1} \tag{3}$$

Assuming the separability of time and space of the vibration modes, $\boldsymbol{x}(t) = \{\boldsymbol{\varphi}\}\boldsymbol{\eta}(t)$, the movement equation takes the form of $[\mathbf{I}]\{\ddot{\boldsymbol{\eta}}(t)\} + 2[\boldsymbol{Z}][\boldsymbol{\Lambda}]\{\dot{\boldsymbol{\eta}}(t)\} + [\boldsymbol{\Lambda}]\{\boldsymbol{\eta}(t)\} = \{\boldsymbol{\varphi}\}^T\{\mathbf{F}(t)\} = \{\mathbf{F}_m(t)\}$, which is a set of uncoupled system of equations. Performing the Fourier transform of the set of equations results in Eq. (4),

$$-\boldsymbol{\omega^2}[\mathbf{I}]\{\boldsymbol{\eta}(\omega)\} + 2i\omega[\boldsymbol{Z}][\boldsymbol{\Lambda}]^{1/2}\{\boldsymbol{\eta}(\omega)\} + [\boldsymbol{\Lambda}]\{\boldsymbol{\eta}(\omega)\} = \{\mathbf{F}_{\boldsymbol{m}}(\boldsymbol{\omega})\} \tag{4}$$

and the transfer function of the system in the modal space is shown in Eq. (5).

$$\{\boldsymbol{\eta}(\omega)\} = [\mathbf{H}_{\boldsymbol{m}}(\omega)]\{\mathbf{F}_{\boldsymbol{m}}(\omega)\} \quad \text{with} \qquad [\mathbf{H}_{\boldsymbol{m}}(\boldsymbol{\omega})] = [-\boldsymbol{\omega^2}[\mathbf{I}] + 2i\boldsymbol{\omega}[\boldsymbol{Z}][\boldsymbol{\Lambda}]^{1/2} + [\boldsymbol{\Lambda}]\,]^{-1} \tag{5}$$

Also, the power spectral density function is defined by $[\mathbf{S}_{\boldsymbol{\eta}}(\omega)] = [\mathbf{H}_{\boldsymbol{m}}(\omega)][\mathbf{S}_{\boldsymbol{Fm}}(\boldsymbol{\omega})][\mathbf{H}_{\boldsymbol{m}}{}^*(\omega)]^T$, with "*" meaning the complex conjugate, $\mathbf{S}_{\boldsymbol{Fm}}$ the power spectral density of the modal forces and $\mathbf{H}_{\boldsymbol{m}}(\omega)$ the transfer function. (Newland, 1984). Back to the space of the actual variables $\boldsymbol{x}(t)$, the Power Spectral density function at the degrees of freedom is obtained by $[\mathbf{S}_{\boldsymbol{x}}(\omega)] = \{\boldsymbol{\varphi}\}[\mathbf{H}_{\boldsymbol{m}}(\omega)]\{\boldsymbol{\varphi}\}^T[\mathbf{S}_{\boldsymbol{F}}(\omega)]\{\boldsymbol{\varphi}\}[\mathbf{H}_{\boldsymbol{m}}{}^*(\omega)]^T\{\boldsymbol{\varphi}\}^T$.

By the autocorrelation function definition and the relation to the power spectral density function, the variance of the process (zero mean), can be estimated by the integration of the Power Spectral Density as indicated by Eq. (6). The integral value is doubled to consider that $[\mathrm{S}_x(\omega)]_{i,i}$ is defined between -∞ e ∞, while the integral is calculated over 0 and ∞.

$$\boldsymbol{E}[\{\boldsymbol{x^2}(t)\}_i] = (1/T)\int_0^T x_i^2(t)dt = (\boldsymbol{x}_{i,rms})^{\boldsymbol{2}} = 2\int_0^\infty [\mathrm{S}_x(\omega)]_{i,i}\; d\omega = \int_0^\infty [\mathrm{G}_x(\omega)]_{i,i}\; d\omega \tag{6}$$

For the derived processes like velocity and acceleration, the corresponding power Spectral Densities are evaluated respectively as $[\mathbf{S}_{\dot{\boldsymbol{x}}}(\omega)] = \omega^2[\mathbf{S}_{\boldsymbol{x}}(\omega)]$ and $[\mathbf{S}_{\ddot{\boldsymbol{x}}}(\omega)] = \omega^4[\mathbf{S}_{\boldsymbol{x}}(\omega)]$**.**

In case of internal stresses of a given finite element, for example, similar equations for the Power Spectral Densities can be derived like $[\boldsymbol{S_\sigma^e}(\omega)] = [\boldsymbol{D^e}][\boldsymbol{B^e}][\boldsymbol{S_x^e}(\omega)][\boldsymbol{B^e}]^{\boldsymbol{T}}[\boldsymbol{D^e}]^{\boldsymbol{T}}$. The same is valid for the support reactions. It should be pointed that information about support reaction histories as well as internal stresses over time and their respective spectral densities are relevant both for the foundations design and fatigue analysis of the wind turbine components.

3.5 Wind velocity modeling

The evaluation of the actions caused by the wind on the structure depends on the precise modeling of its speed values that hit the wind turbine tower. The wind energy spectrum is characterized by two distinct peaks with a long gap between them. The effects that the peaks cause are in macro and microscale. The macro meteorological effects are of global order and caused by the flow of air between systems of pressure created in the atmosphere of the Earth by the differential heating, forming cells of high and low pressure that are yet modified by the Coriolis effect of the Earth's rotation. By the structural point of view, these winds represent the loading that will happen persistently during the turbine's service life. The micrometeorological effects are turbulent gusts caused, mainly, by the friction with the soil and obstacles in the turbine's surroundings. The spectral gap allows the statistics of long and short term to be separated. This way the speed of the wind can be described as the sum of the average and fluctuating parts as indicated by Eq. (7). The average speed ($\bar{U}(z)$) is modeled with the hypothesis of atmospheric boundary layer, making it a function of the height and can be represented in a logarithmic or exponential form, as function of the wind speed at a reference height. In this study, the power form $\bar{U}(z) = u_r(\, z/z_r)^\alpha$ is used.

$$u(y,z,t) = \bar{U}(z) + \tilde{u}(y,z,t) \tag{7}$$

The random characteristic of the wind gusts formation prevents a deterministic treatment of the wind speeds, requiring a statistic study and the spectral density function should be taken into consideration. For the representation of the wind, the most used spectrums are the ones proposed by Kaimal, von Kármán, Harris and Davenport, which are obtained based on the measurement of the wind speed for different topographies and heights. For the von Kármán spectrum, Eq. (8) represents wind velocities as function of frequency in three directions (Simiu and Scanlan, 1996).

$$S_u(f) = \sigma_u^2 \frac{4(\frac{L_i}{U_{z_0}})}{[1+70.8(fL_u/U_{z_0})^2]^{5/6}} \qquad \text{and} \qquad S_j(f) = \sigma_j^2 \frac{4[L_j/U_{z_0}](1+188.4(2fL_j/U_{z_0})^2)}{[1+70.8(fL_u/U_{z_0})^2]^{11/6}} \quad j = v,w \tag{29}$$

U_{z_0} is the average longitudinal speed at the reference height z_0, L_i is the length of the turbulence separation scale of the *i*-th component and f is the frequency in Hertz (Hz). The unit of the spectral density S_u is $(\text{m/s})^2/\text{Hz}$. As shown by Morfiadakis et al. (1996), when compared with measured values for the application in wind farms, the von Kármán spectrum presented a better conformity with the scale and shape of the power spectrum for the free-flow condition. For this reason, the von Kármán spectrum is used in this study, under the hypothesis of a free-flow and stable atmosphere.

3.6 Generation of the correlated wind field

For the generation of the wind field, the algorithm developed by Wang and Cheynet (2018) was used. The method is based on a Monte Carlo simulation (Shinozuka and Jan, 1972). Basically, it indicates that for a random process guided by some spectral density, the sum of non-correlated sinusoidal processes $x(t) = \sum_{i=1}^{nls} \sqrt{2\mathrm{S}_x(\omega_i)\mathrm{d}\omega} \cos(\omega_i t + \varphi_i)$ will generate the desired spectral density, where nls is the number of spectral lines used do discretize the spectral density function and φ_i is a random phase for each frequency.

The spectral field of wind speed history can be generated in two ways: representing wind speed history of one point only and the other is the representation of multiple points. The representation by one point assumes a completely homogenous field, with all the points subjected to the same wind fluctuations. For large structures, the homogenous hypothesis is not realistic, being necessary to relate the fluctuations of speed from one point to another using a correlation function. According to Davenport et al. (1961), the spatial correlation of speeds may be described as a function of the distance *d* between two points and the gusts frequency *f*, *i.e.*, $Coh(d,f) = \exp[-f\sqrt{C_z^2(z_1 - z_2) + C_y^2(y_1 - y_2)}/\bar{U}]$. In this last equation, y_1, y_2, z_1, and z_2 are the coordinates of two points of the side of the structure that is hit by the wind; C_z and C_y are the exponential decay coefficients experimentally obtained. In this study, the coefficient values $C_z = 7$ and $C_y = 10$ are adopted, producing load distributions on the side of safety for the structure.

3.7 Structural wind turbine parameters

The horizontal axis wind turbine has three blades of 30 meters of length. The tower is 60 meters high and has a hollow tapered shape, and is divided into 4 segments of 15 meters each. The diameter of the tower varies linearly from the base, with diameter 3.84m, to the top, with 2.07m, and each segment has different wall-thickness: 0.016m, 0.0125m, 0.0125 and 0.0095m. The wind turbine tower was discretized into 60 beam-type elements, 20 used for the tower, 10 for the

nacelle and 10 for each of the 3 blades, as shown in the Fig. 1b. The nacelle was simplified as a rectangular hollow steel box, with dimensions 1.5x1.5x10 m and wall-thickness 0.08m. The mass of the nacelle's internal elements is 5 tons uniformly distributed along the length of the nacelle. For sake of simplicity, openings and internal elements of the tower were not considered in the simulation. The steel is assumed with 7800 kg/m³ for mass density and 210 GPa for Young Modulus.

3.8 Calculation of the wind action on the structure

In order to calculate the drag force along the tower, the distributed loads were simplified as concentrated loads, obtaining a stepped force along the structure. Taking element *n* as an example, with initial node *i* and final node *j*, the drag force at the nodes *i* and *j* can be calculated as $F_n = A_n C_D(Re)\rho[\overline{U}(z) + \tilde{u}(y,z,t)]^2$, where the area A_n is calculated considering the areas of two adjacent halves to the node *k*, as indicated in the Fig. 2(a). The coefficient values are obtained by interpolation of the experimental curves for the NACA23012 airfoil, used in this work and illustrated in Fig. 2(b).

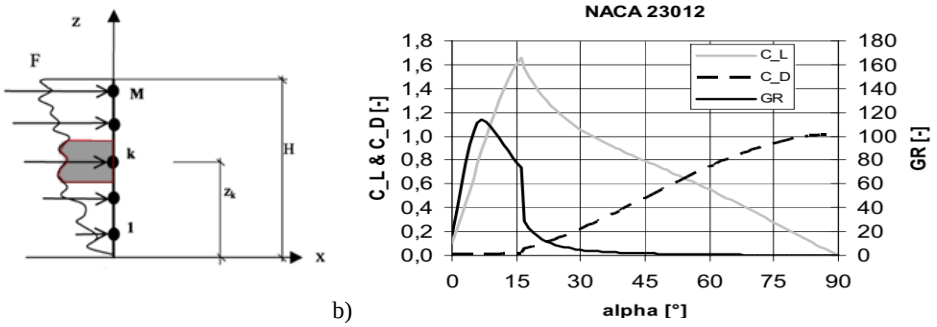

a) b)

Figure 2. a) Steeped wind force approximation. b) Aerodynamic coefficient × angle of attack. (Gundtoft, 2009)

The drag coefficient $C_D(\alpha)$ is a function of the angle of attack α and the Reynolds number for the mean velocity $\overline{U}(z)$ at the height where the wind action is being applied. The force of the wind action on the blades is calculated in terms of the lifting force and the drag force according to aerodynamic principles. The calculation procedure was based on the studies of Jeong et al. (2013). In the local system, it is identified the pitch angle ψ that the chord of the aerogenerator has with the local axis of the element y_L. Also, the angle γ that the relative velocity of the wind V_{rel} has with the same local axis y_L is identified. The relative velocity V_{rel} is the vector composition of the angular velocity of the blade $V_{rel} = [(\omega r)^2 + {V_0}^2]^{1/2}$. The angle of attack of the V_{rel} in relation to the blade profile is defined as $\alpha = \psi + \gamma$. For drag and lift force calculation it follows $F_D = A_p C_D(\alpha)\rho[\overline{U}(z) + \tilde{u}(y,z,t)]$ and $F_L = A_p C_L(\alpha)\,[\overline{U}(z) + \tilde{u}(y,z,t)]$. To evaluate the resulting wind action at the global coordinate system, usual rotations are applied to the local components.

In the frequency domain, the wind velocity power spectrum needs to be transformed into power force spectrum and, according to Simiu and Scanlan (1996), it may be represented with sufficient accuracy based on velocity spectrum information using $S_f(y,z,f) = (\rho C \overline{U}(z) A_n)^2 S_v(y,z,f)$, where C is the resultant drag and/or lift coefficient.

4. RESULTS

Based on the methodology described, the routine implementation was performed in the MATLAB language to allow fast and precise calculations. The methodology is applied to the wind turbine tower presented previously, using two sets of wind data, generated using the stochastic processes described previously, for comparison. The parameters adopted to generate the data of wind forces applied to the structure in this study do not mean to represent any specific location, however, are typical of large Brazilian wind farm installations and intend to offer a basis for the evaluation and comparison of results, using, as it can be noticed, the same average wind speeds but with distinct turbulence parameters. Table 1 shows the parameters used as entry data to generate the wind fields. It is notoriously hard to evaluate or measure the structural damping. For hollow tapered steel towers, there are values reported in the literature for the first four vibration modes that are about 0.0080%, 0.0128%, 0.0320% and 0.1280% and were used in this study.

4.1 Wind velocity

The expected and generated data for the fluctuations equivalent to the turbulent part of the correlated wind field are compared in Fig. 3. It can be observed a good agreement between the coherence data obtained with the generated wind velocity time histories (red dots) and the data prescribed by Von Karman (black line), for various distances (8.4, 21, 38 and 59m). This fact provides confidence that the generated data adhere to the proposed wind power spectral density function. Figure 4 shows the fluctuating velocity history to the nodes of the structure. Scenario B presents turbulence length in each direction that is smaller than scenario A.

Table 1. Entry parameters for the simulation.

Parameter	Scenario A	Scenario B
AVG wind speed (m/s)	25.0	25.0
Reference Height (m)	10.0	10.0
Exponent of the boundary layer α (-)	0.130	0.160
Turbulence length (m)	170(x) 100(y) 35(z)	130(x) 40(y) 10(z)
Std. Deviation of turbulence (m/s)	2.60(x) 2.20(y) 1.56(z)	3.6(x) 2.70(y) 2.1(z)
Simulation time T (s)	50.0	50.0
Time interval Δt (s)	0.005	0.005
Number of spectral lines(*nls*)	5000	5000

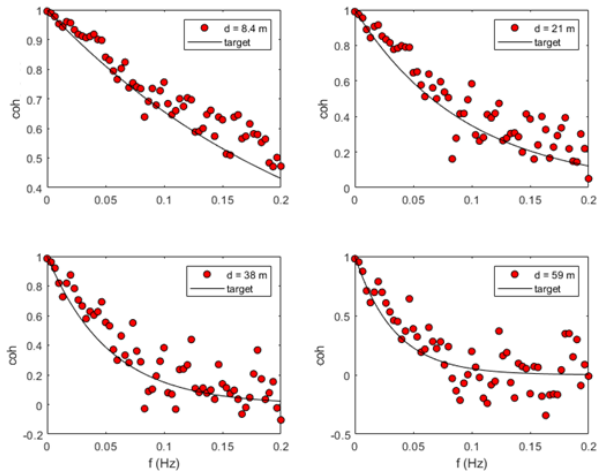

Figure 3. Comparison of the correlation of the wind velocity evaluated by the generated time signal x frequency, for various distances between points (Von Karman model).

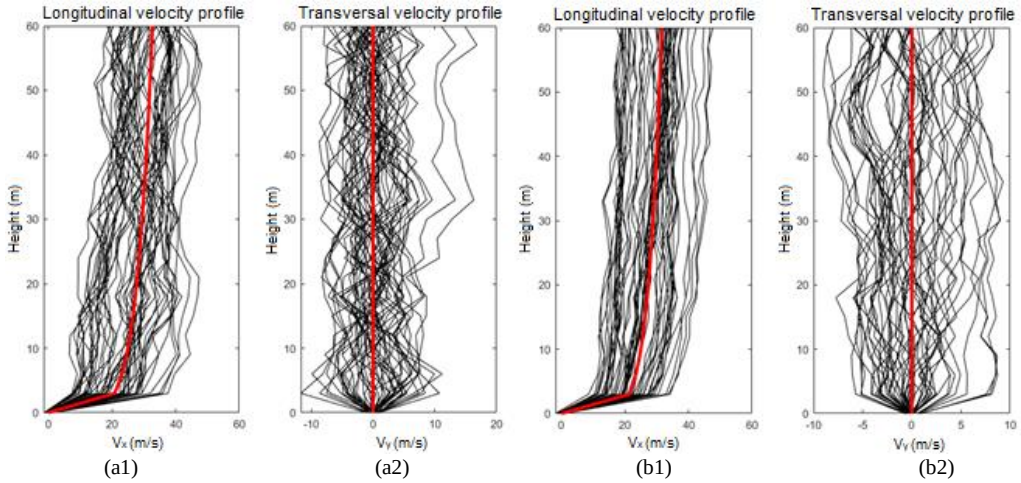

(a1) (a2) (b1) (b2)

Figure 4. Mean wind velocity profile (red) and turbulent velocity profiles (black) in a specific time instant, for (1) longitudinal and (2) transversal wind;(a) stands for scenario A and (b) for scenario B.

Qualitatively, one can see the influence of the correlation function between the graphs of each node, that is, the field is random, but the fluctuations are close to nearby points, which brings significant improvements to the wind speed field, approximating it to reality. A way to evaluate amplitude of the working velocities, Fig. 4 (a) and (b) bring the mean velocity profiles and the turbulent fluctuations to the directions x and y, respectively, as a function of the height for both wind scenarios.

It is important to note in Fig. 4 (a1) and (b1) the amplitude of the wind gusts in relation to the average velocity. In the first case, they have larger variations and, in the second case, they are closer to the mean. It is also noted in the y direction, Fig. 4 (a2) and (b2), that although speed fluctuations (turbulence part) present zero mean, there are already expressive

burst values. These effects are of interest in the structural calculation because they can cause failures even in a condition considered normal, emphasizing the importance of this type of analysis.

4.2 Natural frequencies and mode shapes

As it is a characteristic of the slender structures, the evaluated natural frequency values are low. The 6 first natural frequencies and their respective mode shapes are presented in Fig. 5, being the first two frequencies related to the first lateral and longitudinal bending modes of the whole wind turbine tower. Also, the spectral density of the displacement (G_x) is presented as a function of the frequency in Fig. 6. Notice that the peaks in the spectral density of the structure are precisely the same peaks of the natural frequencies (f_1=0.119 Hz and f_2=0.122 Hz), that is, the structure reacts more intensely in its natural frequencies, according to what was expected, showing the coherence of the model. The other natural frequencies do not appear because, due to the lack of relevant and reliable information, it was considered critical damping for modes higher than the fourth one, as previously described.

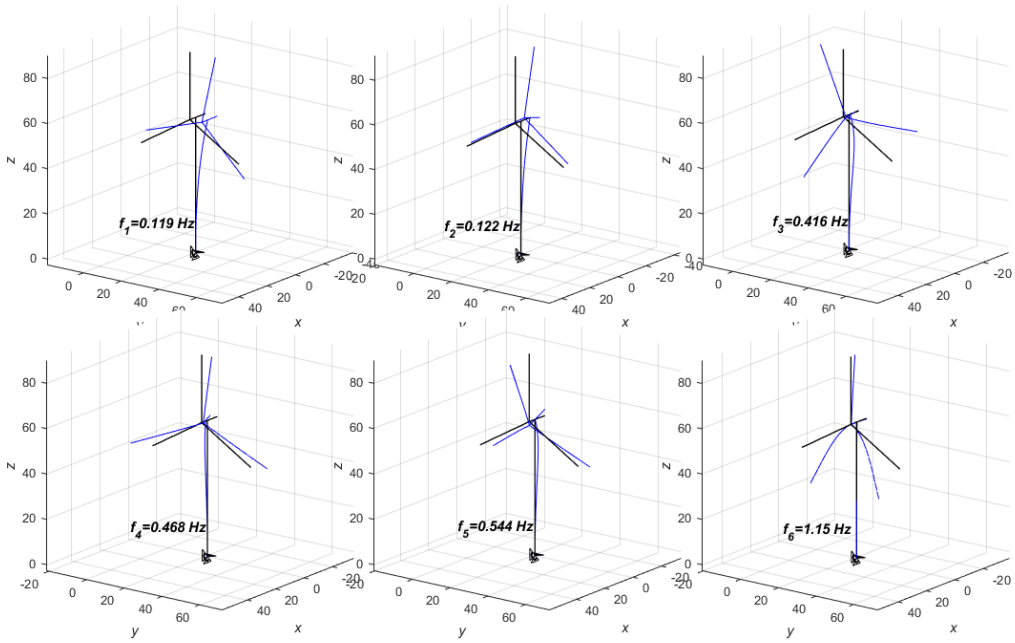

Figure 5. First six natural frequencies and mode shapes of the structure.

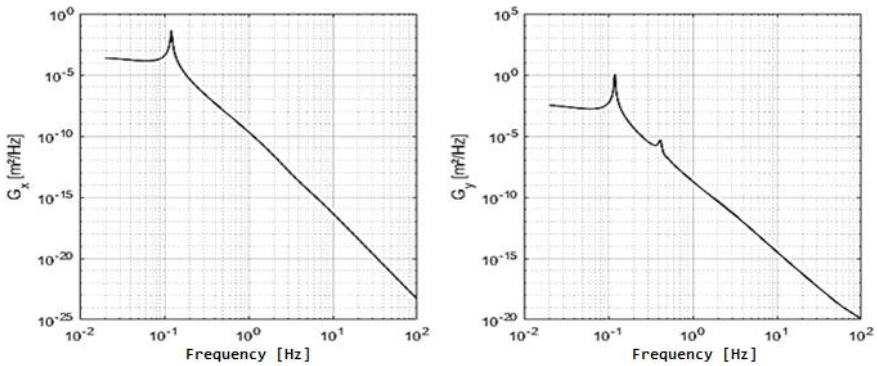

Figure 6. Displacement Power Spectral Density at the top of the tower (node 2): a) longitudinal direction and b) lateral direction. Wind scenario A.

The fact of the natural frequencies being low in this kind of structure is of interest once the gust frequencies of the turbulent portion of the wind present similar frequencies, varying between 0.0055 to 0.2 Hz, and the effects of excitation forces in the same range of the natural frequencies of the structure are notorious. This is highlighted by the Brazilian standard NBR6123 that advices a full dynamic analysis in these cases.

4.3 Comparative analysis of the dynamic response

The numerical analysis, both in time and frequency domains, provide a structural response in terms of Root Mean Square (RMS) values of displacements, velocities, and accelerations at the structure's degrees of freedom. In order to compare the results of the two methodologies, Table 2 presents the resultant RMS values at some critical nodes of the structure for wind scenario A.

Table 2. Values of RMS displacement, acceleration and bending moments on the Wind Turbine Tower.

	Time Domain		Frequency Domain	
Wind Direction	X	Y	X	Y
RMS disp. at the top (m)	0.73205	0.21167	0.72189	0.22351
RMS acc. at the top (m/s²)	0.03933	0.03362	0.03431	0.04223
RMS moment at the bottom (kNm)	110.56	756.41	146.08	738.48
Computational time cost (s)	888.99		858.35	

The similarity of the values found by the two methods in these critical points can be noticed, showing the consistency of the implemented algorithm. The values for RMS acceleration and displacement for this type of wind turbine tower are very similar to those presented by Zendehbad et al. (2017). The computational time durations are also compared and, despite what is said in the literature that the analysis in the frequency domain is computationally more efficient, this was not observed in this case. It was found that the subroutines used to generate the correlated wind speeds field and to generate the power spectral densities were the ones that spent more time in both analysis.

The generation of a complete time series of forces and displacements allows the evaluation of other effects such as fatigue. Figure 7 presents the displacement values obtained in the x and y directions for the heights of 12m, 33m and 60m of the tower.

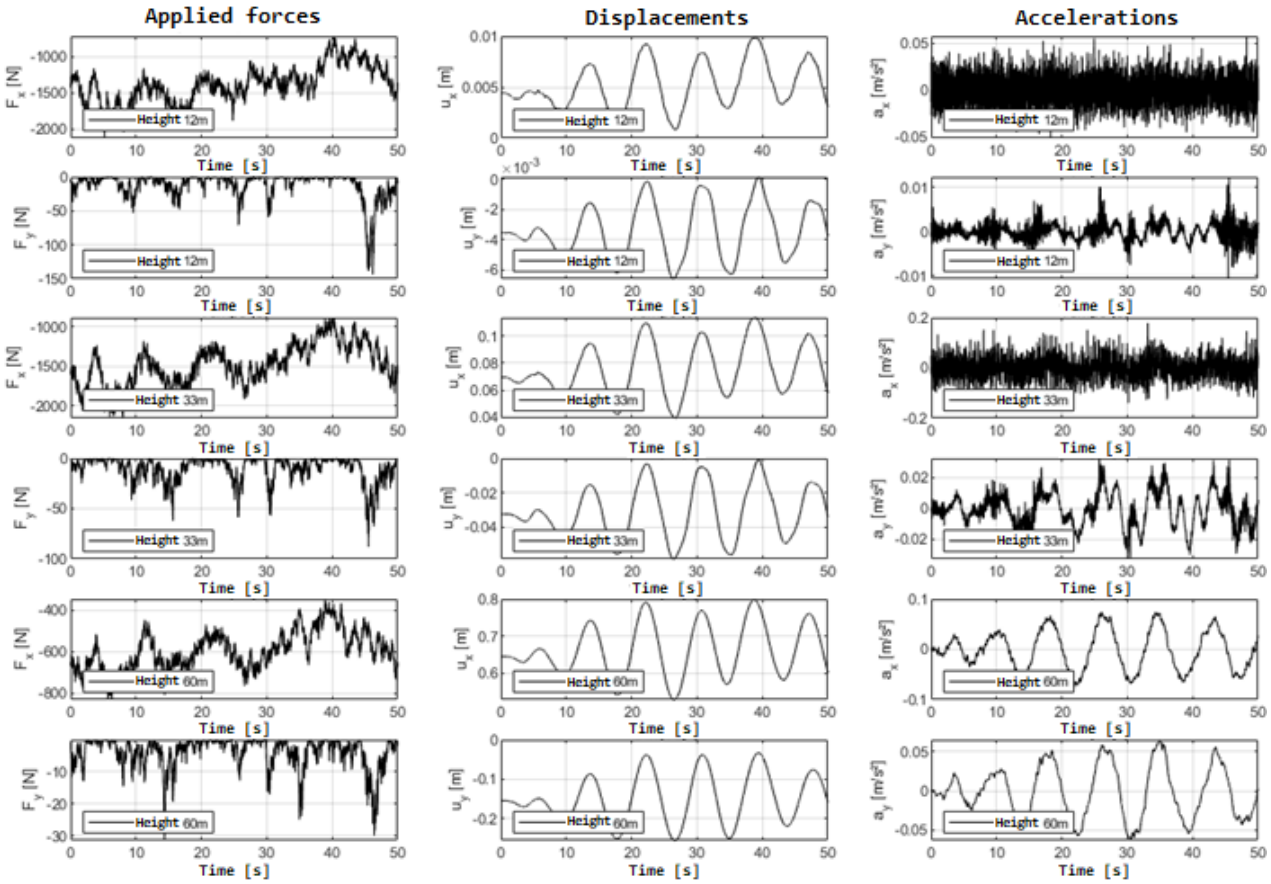

Figure 7. Wind forces on the structure and resultant displacements for different heights of the tower in x and y directions (wind scenario A).

In Figure 7, it can be noticed the recurrent and cyclic feature of the displacements generated on the tower. This is relevant since they can cause failure due to fatigue, considering that this kind of structure has an expected lifespan of 20 to 25 years with regular maintenance.

Also, a pertinent effect that can be observed is the displacement in the transverse (y) direction to the flow, which presents the same shape and period of the displacement in the longitudinal direction, but with reduced amplitude. It means that, in the evaluated state of stopped operation, with the flagged blades and brakes applied, there is displacement and consequently stress in the perpendicular direction to the wind. Given the negligible amplitude of wind loading in this direction, it may be concluded that there must be another cause of this displacement. Analyzing the possible causes, the most probable source of it is the lift force generated by the blade profile tangentially to the rotation direction of the rotor.

It is also verified that the acceleration tends to have higher frequency in the lower elements of the tower, and its frequency, amplitude and period, tend to adjust to that of the force and displacement as the structural rigidity decreases with the height.

4.4 Response in the time domain with distinct scenarios

In order to evaluate the relevance of the turbulent effects, the stresses caused by the two wind conditions presented previously will be compared, since they have been generated with the same average speed, but with different turbulence parameters and terrain roughness. In Fig. 8, the resulting dynamic forces are presented for each condition and the displacements generated by the turbulent wind portion at the top of the tower.

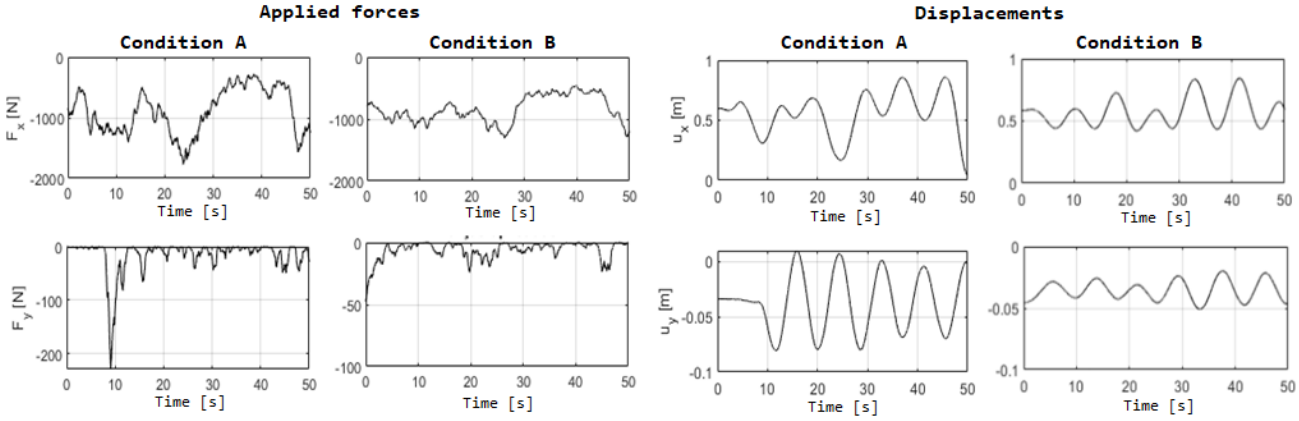

Figure 8. Resultant applied forces and displacements caused by the wind loadings at the top of the tower for the two wind scenarios.

Comparing the results for the two wind scenarios, one can notice a reduction of the RMS values for load and displacement magnitude, for Scenario B, as presented by Tab. 3. The effects are even clearer considering the bending moment and the compression reaction force at the base of the structure. In Fig. 9, it is possible to observe that the difference can be greater than one order of magnitude, and the same happens for shear forces at the first component of the structure near the ground. Therefore, it is clear the influence and relevance that the turbulent portion of the wind has on the tower responses, since the scenario A, with greater turbulence, present considerably greater impact on the structure than scenario B.

Table 3. RMS values of the turbulent loadings for some nodes of the wind turbine tower.

Loadings	**Scenario A**	**Scenario B**	**Var. (%)**
Compression force at the tower's top F_x (kN)	969.17	866.43	12%
Shear force at the tower's top F_y (kN)	34.8700	9.55	265%
Longitudinal Displacement at the tower's top U_x (m)	0.586	0.585	0%
Lateral Displacement at the tower's top U_y(m)	0.0452	0.0364	24%
Long. Bending moment at the tower's base M_x (kNm)	110564.13	68356.87	62%
Lateral Bending moment at the tower's base M_y (kNm)	1838.10	835.84	120%
Compression force at the tower's base F_x (kN)	1002.10	987.68	1%
Shear force at the tower's base F_y (kN)	39.69	24.95	59%

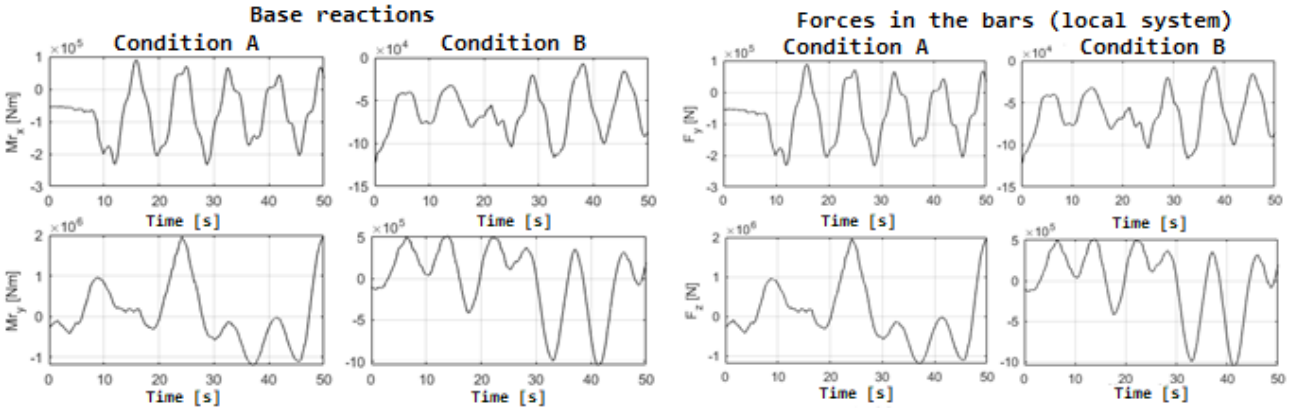

Figure 9. Reactions and forces in some elements as a function of time for the two wind conditions.

These results highlight the importance of the random or turbulent portion of the wind and of the roughness of the terrain for the loadings on the structure and suggests possible discrepancies with methods that use the mean wind velocity as the only parameter of calculation.

5. CONCLUSIONS

The present work proposes a model to simulate the structural behavior of wind turbine towers loaded by wind gusts that are generated as a correlated multipoint spatial field. Developed in the MATLAB programing platform, the routines aimed to evaluate displacements, velocities, accelerations, forces and moments acting on the structure, as well as its natural frequencies and vibration modes. Two wind scenarios, that differ only in the parameters of the random portion of the wind, were compared. It was identified variation in the reaction forces and moments generated, with peaks that exceed one order of magnitude. In the studied case, it was not possible to conclude that the implemented algorithm in the frequency domain has a great computational advantage over the more traditional method of time domain direct integration, however it showed complete coherence for the RMS values evaluated by the time domain integration. For future work, it is foreseen the implementation of optimization algorithms and a fatigue load study.

6. REFERENCES

Ashuri, T., Zaaijer, M., Bussei, G., van Kulk, G. "An analytical model to extract wind turbine blade structural properties for optimization and up-scaling studies", *3rd EWEA Conf. The Science of Making Torque from Wind*. Heraklion, Crete, Greece, 1-7, 2010.

Jeong, M. -S., Lee, I., Yoo, S. -J., Park, K. -C. "Torsional stiffness effects on the dynamic stability of a horizontal axis wind turbine blade". *MDPI*, Basel, Suiss, 2013.

Ma, Y., Martinez-Vazquez, P., Baniotopoulos, C. "Wind turbine tower collapse cases: a historical overview". *Proc. of the Institution of Civil Engineers. Structures and Buildings.* 2018.

Malcolm, D.J., Laird, D.L. "Extraction of equivalent beam properties from blade models". *Wind Energ.*, V.10, pp.135-157, 2007.

Morfiadakis, E.E., Glinou, G.L., Koulouvari, M.J. "The suitability of the von Karman spectrum for the structure of turbulence in a complex terrain wind farm". *J. of Wind Engrg. and Ind. Aerod*, Vol. 62, pp.237-257, 1996.

Newland, D.E. *An introduction to random vibration and spectral analysis*. Longman, 2nd edition. 1984.

Rodríguez, A.G.G., Rodríguez, A.G., Payán, M.B. "Estimating wind turbines mechanical constants", *RE&PQJ*, Vol. 1, No.5, 2007.

Shinokuza, M, Jan, C. M. "Digital simulation of random process and its applications". *Journal of Sound and Vibration*, v. 25-1. pp. 111-128, 1972.

Simiu, E., Scanlan, R.H. *Wind effects on structures: fundamentals and applications to design*. John Wiley and Sons, Inc. New York, 3rd. Ed., 1996.

Wang, J., Cheynet, E., Snæbjörnsson, J. P., Jakobsen, J. B. "Coupled aerodynamic and hydrodynamic response of a long span bridge suspended from floating towers". *J. of Wind Engrg. and Ind. Aerod.*, Vol.177, pp.19-31, 2018.

Zendehbad, M., Chokani, N., Abhari R.S. "Measurements of tower deflections on full-scale wind turbines using an optomechanical platform". *J. of Wind Engrg. and Ind. Aerod*. V.168, pp.72–8. 2017.